DOI: 10.1109/LAWP.2016.2609284

Dynamic Performance of Electrical Balance Duplexing in a Vehicular Scenario

Leo Laughlin, *Member, IEEE,* Chunqing Zhang, *Member, IEEE,* Mark A. Beach, *Member, IEEE,* Kevin A. Morris, *Member, IEEE,* and John L. Haine, *Member, IEEE*

***Abstract*—Electrical Balance Duplexers (EBDs) can achieve high transmit-to-receive (Tx-Rx) isolation, but can be affected by interaction between the antenna and environment. Circuit simulations incorporating measured time-variant antenna impedance data have been used to quantify performance variation and determine circuit adaptation requirements for EBDs operating in vehicular scenarios at 875 MHz and 1900 MHz. Results show that the interaction between the antennas and the external environment is limited and vehicle motion does not necessitate high speed EBD adaptation, however the impedance of dashboard mounted antennas can vary due to interaction with the windscreen wipers, causing substantial variation in the Tx-Rx isolation and requiring EBD re-balancing intervals of 5 ms or less to maintain performance.**

***Index terms*—Duplexers, vehicles, propagation.**

I. Introduction

ELECTRICAL BALANCE DUPLEXERS (EBDs) [1]–[5] provide high transmit-to-receive (Tx-Rx) isolation and can be tuned over wide frequency ranges, and are therefore of interest as a potential alternative to fixed frequency acoustic resonator filters in cellular FDD transceivers (e.g. surface acoustic wave (SAW) filters), which effectively limit the number of bands that can be covered due to the cost, size, and loss associated with these components [6], [7]. EBDs implement a form of self-interference cancellation, and are also of interest as the first stage of cancellation in in-band full-duplex (IBFD) transceivers [3], [8]. IBFD systems typically achieve >100 dB of Tx-Rx isolation, thereby allowing simultaneous transmission and reception on the same frequency to increase spectral efficiency [8].

The EBD consists of a hybrid junction and a tunable *balancing impedance*, connected to the transmitter, receiver, and antenna, as shown in Fig. 1. High transmit to receive isolation is obtained when the balancing impedance is equal to the antenna impedance, however the antenna impedance can be time-variant due to electromagnetic interaction with the local environment, and thus the balancing impedance must also adaptively track the antenna impedance in order to maintain Tx-Rx isolation in dynamic environments. The high levels of isolation achieved (>50 dB) by EBDs are contingent on very close matching between the antenna and balancing reflection coefficients, requiring a balancing impedance tuning resolution of the same order as the required isolation [2], [4]. Furthermore, due to the required balancing accuracy, the circuit can be sensitive to very small variations in the antenna reflection coefficient caused by environmental interactions. Previous contributions on this topic [9], [10] have embedded dynamically measured antenna reflection coefficient data into adaptive EBD circuit simulations to investigate the impact on performance and the requirements for adaptation. Results demonstrate that user interaction and device motion in indoor environments can cause substantial variations in Tx-Rx isolation, but that updating the balancing impedance value at intervals of the order of 10 ms is effective at maintaining isolation in these environments.

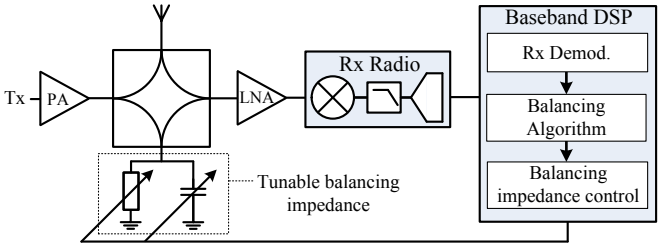

Fig. 1. An EBD with adaptive balancing impedance control.

This letter investigates EBD performance variation and balancing adaptation requirements in vehicular scenarios. Previously measured dynamic environments [9], [10] were slowly changing due to the low speed of user motion and indoor device motion, however the much higher speeds in vehicular scenarios have the potential to require correspondingly faster balancing impedance adaptation. It is therefore necessary to quantify EBD performance for this use case in order that potential limitations can be identified and the dynamic tracking performance specified appropriately. Dynamic antenna reflection coefficient variation of vehicle rooftop and dashboard mounted antennas has been measured at frequencies of 875 MHz and 1900 MHz and for various vehicle speeds up to 112 km h^{-1}. The measured S_{11} time series' were then embedded into EBD circuit simulations to analyze the variation in EBD performance and determine adaptation requirements.

II. Vehicular Antenna Measurements

Three antennas were selected for use in this investigation: a Taoglas PAD710 multiband cellular antenna, and two dipole

Manuscript received March 1st 2016, revised July 24th 2016, accepted August 23rd 2016. This research is supported by the UK EPSRC through the University of Bristol Impact Acceleration Account (EP/K503824/1), and by u-blox AG.

L. Laughlin, C. Zhang, M. A. Beach, K. A. Morris, and J. L. Haine are with the Department of Electrical and Electronic Engineering, University of Bristol, BS8 1UB, UK. e-mail: Leo.Laughlin@bristol.ac.uk.

Digital Object Identifier (DOI):
Data publicly available; DOI: 10.5523/bris.2st0sv04lg2p18tu94pybqftz.

DOI: 10.1109/LAWP.2016.2609284

antennas, one designed for operation at 875 MHz and the other for operation at 1900 MHz. The use of two dipole antennas at two different frequencies allows differences between the final results to be attributed to the differences in propagation behavior only (this is not the case with the multiband cellular antenna as the antenna exhibits different patterns and efficiencies at different frequencies). Two antenna mounting positions were selected: a rooftop antenna position towards the rear of the vehicle and a dashboard mounted antenna (commonly mounted beneath the dashboard cover and therefore not visible). The vehicle used in this investigation was a 5-door Vauxhall Astra, this being an average sized European car. The vehicle did not have metalized tinted windows or an electrically heated front windscreen.

Antenna reflection coefficient measurements were performed across two 20 MHz bandwidths centered at 875 MHz and 1900 MHz. This measurement bandwidth was chosen as the simulated EBD (described in the following section) operates over a 20 MHz bandwidth, this being the largest bandwidth used by long term evolution (LTE). Each measurement/simulation operates over a single contiguous 20 MHz band, corresponding to an IBFD system, however since the tunable balancing impedances presented in [4], [11] allow for simultaneous *independent* impedance control in the uplink and downlink bands this analysis is also directly relevant to the FDD application.

The antenna S_{11} measurements were performed using a National Instruments vector signal transceiver (VST) system configured as a vector network analyzer (VNA), measuring the antenna S_{11} across a 20 MHz bandwidth with a frequency resolution of 100 kHz at 0.5 ms intervals (i.e. 2 kHz sampling rate). The maximum Doppler spread of the dynamic antenna S_{11} which can be captured alias free is therefore 2 kHz. This corresponds to a maximum Doppler shift of 1 kHz, which at At 1900 MHz corresponds to a maximum speed of 158 m s^{-1} (568 km h^{-1}), which is sufficient for car based measurements. Measurements were taken at vehicle speeds from 0 to 48 km h^{-1} in a dense urban environment, and at speeds from 0 to 112 km h^{-1} in a motorway environment. Measurements were also taken a slow speeds (<10 km h^{-1}) in an underground carpark environment.

III. Simulated Adaptive EBD

Frequency domain variation in the antenna reflection coefficient is the primary factor limiting EBD isolation [3]. Incorporating a measured antenna S_{11} into a basic circuit simulation can therefore provide an accurate evaluation of the Tx-Rx frequency response of the EBD, and this hybrid measurement/simulation methodology has been validated against hardware measurements [9]. The antenna S_{11} measurements described above provide a time series of antenna reflection coefficient frequency responses. This is incorporated into an EBD circuit simulation to provide a highly realistic time-frequency model of the dynamic antenna reflection coefficient. The EBD simulation assumes an ideal hybrid junction and ideal lumped element components in the tunable balancing impedance circuit. The simulated balancing impedance circuit is a parallel resistor capacitor (RC) or resistor inductor (RL) depending on whether the measured antenna exhibits capacitive or inductive reactance[1], and includes a transmission line matched to the mean group delay of the antenna and interconnect.

(a) (b)

Fig. 2. The 1900 MHz dipole mounted on the (a) dashboard and (b) rooftop. Calibration standard used for in-situ VNA calibration can also be seen in (b).

The level of isolation provided by an EBD is determined by the limited accuracy with which the single pole balancing circuit can mimic the antenna impedance *across the whole band* [3]. This limits the isolation bandwidth, thereby also limiting the average isolation across a particular bandwidth, however the isolation across a given band can be maximized by applying the minimum mean squared error (MMSE) technique presented in [3], thereby minimizing total self-interference power. To balance the duplexer, the simulation calculates the optimal component values directly from the antenna S_{11} data. In a practical system the same result can be achieved using the *balancing algorithm* presented in [5]. The simulation applies this MMSE technique to maximize isolation, and reports the mean isolation across the band, I, as a function of discrete time according to the following expression

$$I(nT_s) = \left(\frac{1}{K} \sum_{k=0}^{K-1} \left| \hat{G}[k, nT_s] \right|^2 \right)^{-1} \quad (1)$$

where $\hat{G}[k, nT_s]$ is the Tx-Rx transfer function of the simulated duplexer at time $t = nT_s$, T_s is the measurement/simulation sampling period (0.5 ms), and the interval $k \in [0, K-1]$ represents the measurement frequencies within the 20 MHz band of interest. The average isolation across the band is an appropriate metric, as this determines the Rx signal to interference ratio. As was the case in [9] and [10], the simulation implements three balancing impedance adaptation characteristics. *Ideal balancing* calculates new balancing impedance component values on every simulation time-step (i.e. for each antenna S_{11} measurement in the time series) thus ensuring the EBD isolation is always maximized. *Static balancing* calculates balancing impedance settings based on the first antenna S_{11} measurement in the time series, but then does not update these values for the remainder of the simulation duration. *Limited rate adaptation* (LRA) recalculates balancing impedance settings at a given interval (i.e. according to every n^{th} measurement in the antenna S_{11} time series). These three adaptation behaviours allow the degradation in isolation

[1]Tunable inductors are impractical in this application, however in practice a tunable inductance can be emulated over a limited frequency and tuning range using a fixed inductor in parallel with a tunable capacitor, as shown in [12].

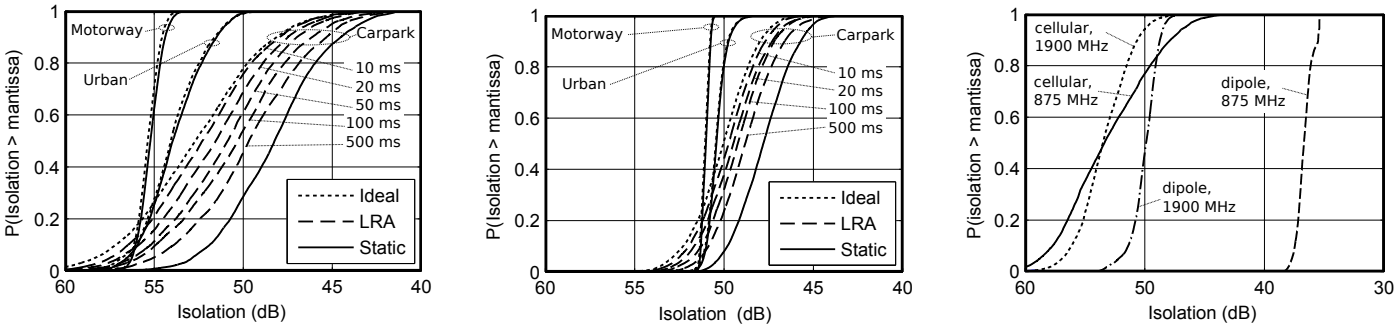

(a) 875 MHz, dipole, roof. (b) 1900 MHz, dipole, roof. (c) Carpark, LRA (10 ms), dashboard.

Fig. 3. Cumulative distribution functions of the simulated Tx-Rx isolation. (a): rooftop dipole antenna in the three measured environments at 875 MHz and when using ideal, static, and limited rate adaptation (LRA) for re-balancing intervals between 10 ms and 500 ms. (b): same as (a) but at 1900 MHz. (c) Comparison of dashboard mounted antennas when using LRA with re-balancing interval of 10 ms in the carpark environment.

due to imperfect balancing adaptation to be quantified and the trade-off between the EBD re-balancing rate and Tx-Rx isolation to be observed. The duration of each simulation run is approximately 10 s (as determined by the duration of the S_{11} time series which is input to the simulation). Simulations of a longer duration were observed to give substantially identical results, demonstrating that a duration of several seconds is adequate to capture the range of variation of the dynamic antenna reflection coefficient in the measured environments. A more detailed description of this simulation method can be found in [10].

IV. Results

A. Interaction with exterior environment

The cumulative distribution functions (CDFs) of the simulated Tx-Rx isolation over the duration of various EBD circuit simulations are plotted in Fig. 3. Fig. 3a and Fig. 3b compare the results from the three dynamic environment scenarios: the motorway at a speed of approximately 112 km h^{-1}, the urban environment at a speed of approximately 32 km h^{-1}, and the underground carpark at a speed of approximately 10 km h^{-1}. Results are plotted for the ideal and static balancing impedance adaptation behaviors, and for limited rate balancing impedance adaptation with balancing intervals of 10-500 ms, as annotated. In the outdoor environments (motorway and urban) it is notable that the resulting isolation from ideal and static balancing are very similar, demonstrating that *balancing impedance adaptation is not critical to Tx-Rx isolation performance in these scenarios.* Since the static case achieved close to ideal performance, curves for LRA are not plotted for these environments. It can be seen that the Tx-Rx isolation is slightly lower and is more variable in the urban environment as compared to the motorway, and this can attributed to the increased environmental reflection in this environment, however the difference is relatively small. In the carpark environment, substantially more variation is observed. For the roof mounted dipole at 875 MHz (Fig. 3a), even when EBD balancing is ideal, there is >15 dB variation in the Tx-Rx isolation at 875 MHz. In this environment there is also a larger difference between the ideal and static case, demonstrating that the increased environmental reflection reduces the EBD performance, however even in this environment the loss in performance is limited to, on average, approximately 5 dB. Comparing results from the carpark environment at the two different frequencies (Fig. 3a and Fig. 3b), it is also clear that the environmental reflections cause greater variation at the lower frequency. This can be attributed to the reduced propagation loss experienced by the lower frequency signal, which means that environmental reflections will have a greater impact on the antenna reflection coefficient. As would be expected given the larger variation in Tx-Rx isolation, the range of variation in the antenna reflection coefficient itself was also observed to be largest in the carpark at 875 MHz. In this scenario all antenna reflection coefficient measurements exhibited a voltage standing wave ratio (VSWR) of less than 1.85:1. The simulated balancing reflection coefficient required a corresponding tuning range.

Similar results were observed for the other antennas/positions, with the variation in Tx-Rx isolation being small in the motorway and urban environments regardless of the antenna type, position and frequency. Fig. 3c plots results for the dashboard mounted antennas when using LRA with a 10 ms re-balancing interval in the carpark environment. Comparing the results for dashboard mounted dipole antennas against rooftop mounted dipoles (as shown in Fig. 3a and Fig. 3b), It can be seen that EBD performance is reduced in the dashboard mounted scenario. At 1900 MHz the reduction is only 2-3 dB, however at 875 MHz a substantial reduction in EBD isolation is observed, demonstrating that objects in close proximity to the antenna can have a substantial detrimental impact on EBD performance. The cellular antennas were observed to result in slightly better performance in this environment.

B. Interaction with vehicle and passengers

For dashboard mounted antennas, vehicle motion is not the only source of environmental variation: the passengers and moving vehicle parts may also perturb the antenna reflection coefficient. To quantify these effects, measurements were also conducted in a further two scenarios: whilst the driver was adjusting the vehicle controls and moving the steering

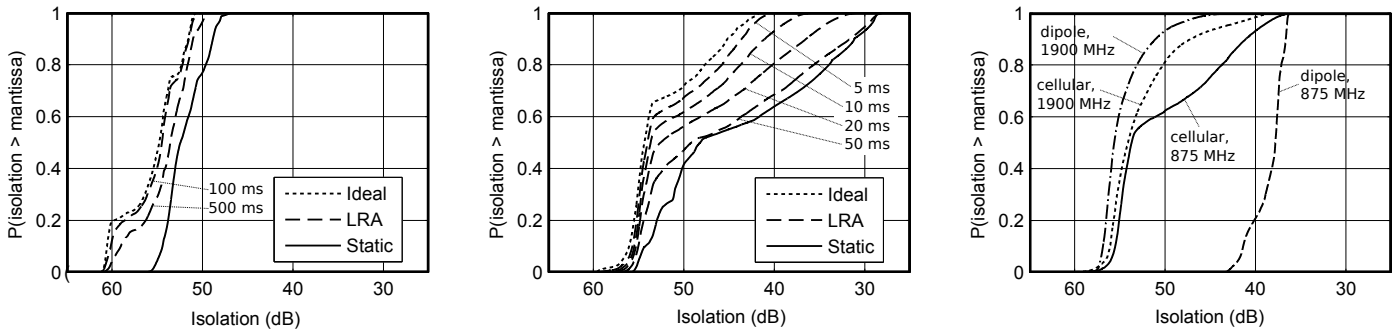

(a) Driver interaction, 875 MHz, cellular antenna. (b) Wipers on, 875 MHz, cellular antenna. (c) Wipers on, LRA (10 ms).

Fig. 4. Cumulative distribution functions of the simulated Tx-Rx isolation. (a): Driver interaction at 875 MHz with the cellular antenna when using ideal, static, and LRA for re-balancing intervals of 100 ms and 500 ms. (b): With windscreen wipers on using the cellular antenna at 875 MHz for ideal, static, and LRA for re-balancing intervals between 5 ms and 50 ms. (c) Comparison of different antennas/frequencies when using a 10 ms re-balancing interval with wipers on.

wheel (emulating normal driving behaviour), and whilst the windscreen wipers were switched on[2]. The range of variation in the antenna reflection coefficient was significantly higher in this scenario, with the windscreen wipers resulting in the largest variations. Due to the relatively poor matching of the cellular antenna, and detuning from environmental interaction, the VSWR of the antenna reflection coefficient was observed to go as high as 3.6:1. The corresponding simulation results are plotted in Fig. 4. The effect of driver interaction is plotted in Fig. 4a for the cellular antenna at 875 MHz, showing that *the impact of the driver/passengers is limited*, and that a 100 ms re-balancing interval is sufficient to maintain near ideal isolation in this scenario. However, as shown in Fig. 4b, the windscreen wipers were observed to induce large reductions in the duplexer isolation. Without adaptation (i.e. static balancing), the isolation was observed to fall below 30 dB at times, and a relatively fast re-balancing interval of 5 ms was required to maintain performance to within 3 dB of the ideal EBD. This results demonstrates that, *adaptive EBD balancing can be critical to Tx-Rx isolation for dashboard mounted antennas*. However, Fig. 4c shows that the degradation is less severe in the higher frequency antennas, attributable to the smaller near-field region of these devices.

V. Conclusion

Circuit simulations which include measured time-variant antenna impedance data have been used to quantify performance variation and determine balancing impedance adaptation requirements for electrical balance duplexers operating in vehicular scenarios. Results show that vehicle motion does not necessitate high speed EBD adaptation, but dashboard mounted antennas are susceptible to interaction with the windscreen wipers, requiring re-balancing intervals of 5 ms or less to maintain Tx-Rx isolation.

[2]For the results in IV.A the driver/passengers were remaining as still as possible whilst each measurement was recorded and the wipers were off. The driver was wearing a metallic wrist watch on the wrist closest to the antenna.

Acknowledgments

The Authors thank Ken Stevens, Steve Gibbs and Peter Bagot for their assistance, and Toaglas for providing the cellular antenna.

References

[1] M. Mikhemar, H. Darabi, and A. A. Abidi, "A Multiband RF Antenna Duplexer on CMOS: Design and Performance," *Solid-State Circuits, IEEE J.*, vol. 48, no. 9, pp. 2067–2077, 2013.

[2] S. H. Abdelhalem, P. S. Gudem, and L. E. Larson, "Hybrid Transformer-Based Tunable Differential Duplexer in a 90-nm CMOS Process," *Microw. Theory Tech. IEEE Trans.*, vol. 61, no. 3, pp. 1316–1326, 2013.

[3] L. Laughlin, M. A. Beach, K. A. Morris, and J. L. Haine, "Optimum Single Antenna Full Duplex Using Hybrid Junctions," *IEEE J. Sel. Areas Commun.*, vol. 32, no. 9, pp. 1653–1661, Sep. 2014.

[4] B. vanLiempd, J. Craninckx, R. Singh, P. Reynaert, S. Malotaux, and J. R. Long, "A Dual-Notch +27dBm Tx-Power Electrical-Balance Duplexer," in *ESSCIRC 2014 - 40th Eur. Solid State Circuits Conf.* IEEE, Sep. 2014, pp. 463–466.

[5] L. Laughlin, C. Zhang, M. A. Beach, K. A. Morris, and J. L. Haine, "Passive and Active Electrical Balance Duplexers," *IEEE Trans. Circuits Syst. II Express Briefs*, vol. 63, no. 1, pp. 94–98, Jan. 2016.

[6] R. Aigner, "Tunable Filters? Reality Check! Foreseeable Trends in System Architecture for Tunable RF Filters," *IEEE Microw. Mag.*, vol. 16, no. 7, pp. 82–88, Aug. 2015.

[7] J. Tsutsumi, M. Seth, A. S. Morris III, R. B. Staszewski, and G. Hueber, "Cost-Efficient, High-Volume Transmission: Advanced Transmission Design and Architecture of Next Generation RF Modems and Front-Ends," *IEEE Microw. Mag.*, vol. 16, no. 7, pp. 26–45, Aug. 2015.

[8] A. Sabharwal, P. Schniter, D. Guo, D. W. Bliss, S. Rangarajan, and R. Wichman, "In-Band Full-Duplex Wireless: Challenges and Opportunities," *IEEE J. Sel. Areas Commun.*, vol. 32, no. 9, pp. 1637–1652, Sep. 2014.

[9] L. Laughlin, M. A. Beach, K. A. Morris, and J. L. Haine, "Electrical balance duplexing for small form factor realization of in-band full duplex," *IEEE Commun. Mag.*, vol. 53, no. 5, pp. 102–110, May 2015.

[10] ——, "Electrical Balance Duplexer Adaptation in Indoor Mobile Scenarios," in *Proc. Eur. Conf. Antennas Propag.*, 2015.

[11] S. H. Abdelhalem, P. S. Gudem, and L. E. Larson, "Tunable CMOS Integrated Duplexer With Antenna Impedance Tracking and High Isolation in the Transmit and Receive Bands," *IEEE Trans. Microw. Theory Tech.*, vol. 62, no. 9, pp. 2092–2104, Sep. 2014.

[12] Q. Gu, J. R. De Luis, A. S. Morris, and J. Hilbert, "An Analytical Algorithm for Pi-Network Impedance Tuners," *IEEE Trans. Circuits Syst. I Regul. Pap.*, vol. 58, no. 12, pp. 2894–2905, Dec. 2011.